ISSN 1948-0210 (online)

World Journal of *Stem Cells*

World J Stem Cells 2021 October 26; 13(10): 1360-1609

Published by Baishideng Publishing Group Inc

WJSC

World Journal of Stem Cells

Contents

Monthly Volume 13 Number 10 October 26, 2021

REVIEW

1360 Translational products of adipose tissue-derived mesenchymal stem cells: Bench to bedside applications

Sharma S, Muthu S, Jeyaraman M, Ranjan R, Jha SK

1382 Unveiling the morphogenetic code: A new path at the intersection of physical energies and chemical signaling

Tassinari R, Cavallini C, Olivi E, Taglioli V, Zannini C, Ventura C

1394 Alternative RNA splicing in stem cells and cancer stem cells: Importance of transcript-based expression analysis

Ebrahimie E, Rahimirad S, Tahsili M, Mohammadi-Dehcheshmeh M

1417 SOX transcription factors and glioma stem cells: Choosing between stemness and differentiation

Stevanovic M, Kovacevic-Grujicic N, Mojsin M, Milivojevic M, Drakulic D

1446 Retina stem cells, hopes and obstacles

German OL, Vallese-Maurizi H, Soto TB, Rotstein NP, Politi LE

1480 Considerations for the clinical use of stem cells in genitourinary regenerative medicine

Caneparo C, Sorroza-Martinez L, Chabaud S, Fradette J, Bolduc S

1513 Age and genotype dependent erythropoietin protection in COVID-19

Papadopoulos KI, Sutheesophon W, Manipalviratn S, Aw TC

MINIREVIEWS

1530 Overview of nutritional approach in hematopoietic stem cell trans-plantation: COVID-19 update

Akbulut G, Yesildemir O

1549 Stem cell therapy and diabetic erectile dysfunction: A critical review

Pakpahan C, Ibrahim R, William W, Faizah Z, Juniastuti J, Lusida MI, Oceandy D

1564 Current knowledge on the multiform reconstitution of intestinal stem cell niche

Xu ZY, Huang JJ, Liu Y, Zhao Y, Wu XW, Ren JA

ORIGINAL ARTICLE

Basic Study

1580 Effect of glycyrrhizic acid and 18β-glycyrrhetinic acid on the differentiation of human umbilical cord-mesenchymal stem cells into hepatocytes

Fatima A, Malick TS, Khan I, Ishaque A, Salim A

1595 Impact of senescence on the transdifferentiation process of human hepatic progenitor-like cells

Bellanti F, di Bello G, Tamborra R, Amatruda M, Lo Buglio A, Dobrakowski M, Kasperczyk A, Kasperczyk S, Serviddio G, Vendemiale G

World Journal of Stem Cells

Monthly Volume 13 Number 10 October 26, 2021

Contents

ABOUT COVER

Editorial Board Member of *World Journal of Stem Cells*, Hong-Cui Cao, MD, PhD, Professor, Vice Director, State Key Laboratory for Diagnosis and Treatment of Infectious Diseases, The First Affiliated Hospital, Zhejiang University School of Medicine, No. 79 Qingchun Road, Hangzhou 310003, Zhejiang Province, China. hccao@zju.edu.cn

AIMS AND SCOPE

The primary aim of *World Journal of Stem Cells* (*WJSC*, *World J Stem Cells*) is to provide scholars and readers from various fields of stem cells with a platform to publish high-quality basic and clinical research articles and communicate their research findings online. *WJSC* publishes articles reporting research results obtained in the field of stem cell biology and regenerative medicine, related to the wide range of stem cells including embryonic stem cells, germline stem cells, tissue-specific stem cells, adult stem cells, mesenchymal stromal cells, induced pluripotent stem cells, embryonal carcinoma stem cells, hemangioblasts, lymphoid progenitor cells, *etc*.

INDEXING/ABSTRACTING

The *WJSC* is now indexed in Science Citation Index Expanded (also known as SciSearch®), Journal Citation Reports/Science Edition, Biological Abstracts, BIOSIS Previews, Scopus, PubMed, and PubMed Central. The 2021 Edition of Journal Citation Reports® cites the 2020 impact factor (IF) for *WJSC* as 5.326; IF without journal self cites: 5.035; 5-year IF: 4.956; Journal Citation Indicator: 0.55; Ranking: 14 among 29 journals in cell and tissue engineering; Quartile category: Q2; Ranking: 72 among 195 journals in cell biology; and Quartile category: Q2. The *WJSC*'s CiteScore for 2020 is 3.1 and Scopus CiteScore rank 2020: Histology is 31/60; Genetics is 205/325; Genetics (clinical) is 64/87; Molecular Biology is 285/382; Cell Biology is 208/279.

RESPONSIBLE EDITORS FOR THIS ISSUE

Production Editor: *Yan-Xia Xing*; **Production Department Director:** *Yu-Jie Ma*; **Editorial Office Director:** *Ze-Mao Gong*.

NAME OF JOURNAL
World Journal of Stem Cells

ISSN
ISSN 1948-0210 (online)

LAUNCH DATE
December 31, 2009

FREQUENCY
Monthly

EDITORS-IN-CHIEF
Shengwen Calvin Li, Tong Cao, Carlo Ventura

EDITORIAL BOARD MEMBERS
https://www.wjgnet.com/1948-0210/editorialboard.htm

PUBLICATION DATE
October 26, 2021

INSTRUCTIONS TO AUTHORS
https://www.wjgnet.com/bpg/gerinfo/204

GUIDELINES FOR ETHICS DOCUMENTS
https://www.wjgnet.com/bpg/GerInfo/287

GUIDELINES FOR NON-NATIVE SPEAKERS OF ENGLISH
https://www.wjgnet.com/bpg/gerinfo/240

PUBLICATION ETHICS
https://www.wjgnet.com/bpg/GerInfo/288

PUBLICATION MISCONDUCT
https://www.wjgnet.com/bpg/gerinfo/208

ARTICLE PROCESSING CHARGE
https://www.wjgnet.com/bpg/gerinfo/242

STEPS FOR SUBMITTING MANUSCRIPTS
https://www.wjgnet.com/bpg/GerInfo/239

ONLINE SUBMISSION
https://www.f6publishing.com

World Journal of Stem Cells

Submit a Manuscript: https://www.f6publishing.com

World J Stem Cells 2021 October 26; 13(10): 1595-1609

DOI: 10.4252/wjsc.v13.i10.1595

ISSN 1948-0210 (online)

ORIGINAL ARTICLE

Basic Study

Impact of senescence on the transdifferentiation process of human hepatic progenitor-like cells

Francesco Bellanti, Giorgia di Bello, Rosanna Tamborra, Marco Amatruda, Aurelio Lo Buglio, Michał Dobrakowski, Aleksandra Kasperczyk, Sławomir Kasperczyk, Gaetano Serviddio, Gianluigi Vendemiale

ORCID number: Francesco Bellanti 0000-0002-8196-7373; Giorgia di Bello 0000-0002-8251-3840; Rosanna Tamborra 0000-0003-4790-8529; Marco Amatruda 0000-0002-5407-238Y; Aurelio Lo Buglio 0000-0003-1569-3658; Michał Dobrakowski 0000-0001-8399-7624; Aleksandra Kasperczyk 0000-0002-2035-0388; Sławomir Kasperczyk 0000-0001-8974-5786; Gaetano Serviddio 0000-0002-6424-7841; Gianluigi Vendemiale 0000-0002-7951-0219.

Author contributions: Bellanti F and Vendemiale G designed and coordinated the study; Bellanti, F, di Bello G, Tamborra R, Lo Buglio A, Amatruda M, Dobrakowsky M, and Kasperczyk A performed the experiments, acquired, and analyzed data; Bellanti, F, di Bello G, Tamborra R, Amatruda M, Lo Buglio A, Dobrakowsky M, Kasperczyk A, Kasperczyk S, Serviddio G, and Vendemiale G interpreted the data; Bellanti F wrote the manuscript; Kasperczyk S, Serviddio G, and Vendemiale G supervised the manuscript; All authors approved the final version of the article.

Institutional review board statement: The study was reviewed and approved by the Institutional Review Board at the University of Foggia.

Francesco Bellanti, Giorgia di Bello, Rosanna Tamborra, Marco Amatruda, Aurelio Lo Buglio, Gaetano Serviddio, Gianluigi Vendemiale, Department of Medical and Surgical Sciences, University of Foggia, Foggia 71122, Italy

Michał Dobrakowski, Aleksandra Kasperczyk, Sławomir Kasperczyk, Department of Biochemistry, Medical University of Silesia, Zabrze 41-808, Poland

Corresponding author: Francesco Bellanti, MD, PhD, Doctor, Associate Professor, Department of Medical and Surgical Sciences, University of Foggia, viale Pinto 1, Foggia 71122, Italy. francesco.bellanti@unifg.it

Abstract

BACKGROUND

Senescence is characterized by a decline in hepatocyte function, with impairment of metabolism and regenerative capacity. Several models that duplicate liver functions *in vitro* are essential tools for studying drug metabolism, liver diseases, and organ regeneration. The human HepaRG cell line represents an effective model for the study of liver metabolism and hepatic progenitors. However, the impact of senescence on HepaRG cells is not yet known.

AIM

To characterize the effects of senescence on the transdifferentiation capacity and mitochondrial metabolism of human HepaRG cells.

METHODS

We compared the transdifferentiation capacity of cells over 10 (passage 10 [P10]) *vs* P20. Aging was evaluated by senescence-associated (SA) beta-galactosidase activity and the comet assay. HepaRG transdifferentiation was analyzed by confocal microscopy and flow cytometry (expression of cluster of differentiation 49a [CD49a], CD49f, CD184, epithelial cell adhesion molecule [EpCAM], and cytokeratin 19 [CK19]), quantitative PCR analysis (expression of albumin, cytochrome P450 3A4 [CYP3A4], γ-glutamyl transpeptidase [γ-GT], and carcinoembryonic antigen [CEA]), and functional analyses (albumin secretion, CYP3A4, and γ-GT). Mitochondrial respiration and the ATP and nicotinamide adenine dinucleotide (NAD^+)/NAD with hydrogen (NADH) content were also measured.

Conflict-of-interest statement: All authors have nothing to disclose.

Data sharing statement: No additional data are available.

Manuscript source: Invited manuscript

Specialty type: Gastroenterology and hepatology

Country/Territory of origin: Italy

Peer-review report's scientific quality classification

Grade A (Excellent): 0
Grade B (Very good): 0
Grade C (Good): C
Grade D (Fair): 0
Grade E (Poor): 0

Received: April 26, 2021
Peer-review started: April 26, 2021
First decision: May 12, 2021
Revised: June 14, 2021
Accepted: August 23, 2021
Article in press: August 23, 2021
Published online: October 26, 2021

P-Reviewer: Chen S
S-Editor: Wu XYJ
L-Editor: Filipodia
P-Editor: Wang LYT

RESULTS

SA β-galactosidase staining was higher in P20 than P10 HepaRG cells; in parallel, the comet assay showed consistent DNA damage in P20 HepaRG cells. With respect to P10, P20 HepaRG cells exhibited a reduction of CD49a, CD49f, CD184, EpCAM, and CK19 after the induction of transdifferentiation. Furthermore, lower gene expression of albumin, CYP3A4, and γ-GT, as well as reduced albumin secretion capacity, CYP3A4, and γ-GT activity were reported in transdifferentiated P20 compared to P10 cells. By contrast, the gene expression level of CEA was not reduced by transdifferentiation in P20 cells. Of note, both cellular and mitochondrial oxygen consumption was lower in P20 than in P10 transdifferentiated cells. Finally, both ATP and NAD^+/NADH were depleted in P20 cells with respect to P10 cells.

CONCLUSION

SA mitochondrial dysfunction may limit the transdifferentiation potential of HepaRG cells, with consequent impairment of metabolic and regenerative properties, which may alter applications in basic studies.

Key Words: Senescence; HepaRG cells; Transdifferentiation; Mitochondria; Regeneration; Nicotinamide adenine dinucleotide

Core Tip: The human HepaRG cell line represents an effective model for the study of liver metabolism and hepatic progenitors. However, the impact of senescence on HepaRG cells is not known. We characterized the effects of senescence on the transdifferentiation capacity and mitochondrial metabolism of HepaRG cells. By using a replication protocol, we described higher senescence-associated markers and lower transdifferentiation markers in passage 20 (P20) than in P10 cells. Cellular and mitochondrial oxygen consumption, and ATP and nicotinamide adenine dinucleotide (NAD^+)/NAD with hydrogen (NADH) content were lower in P20 than in P10 transdifferentiated cells. To conclude, senescence-associated mitochondrial dysfunction may limit the transdifferentiation potential of HepaRG cells.

Citation: Bellanti F, di Bello G, Tamborra R, Amatruda M, Lo Buglio A, Dobrakowski M, Kasperczyk A, Kasperczyk S, Serviddio G, Vendemiale G. Impact of senescence on the transdifferentiation process of human hepatic progenitor-like cells. *World J Stem Cells* 2021; 13(10): 1595-1609
URL: https://www.wjgnet.com/1948-0210/full/v13/i10/1595.htm
DOI: https://dx.doi.org/10.4252/wjsc.v13.i10.1595

INTRODUCTION

Primary human hepatocytes are the gold standard to study the biology, pharmacology, and toxicology of parenchymal liver cells[1]. Nevertheless, primary hepatocytes present with several limitations such as difficult isolation procedures, high variability between different donors, quick failure in biological function, and proliferation capacity[2]. To overcome these limitations, several human hepatoma cell lines were developed and characterized to provide a steady and unrestricted supply of hepatocyte-like cells. Of these, HepG2 and Huh-7 cells are the most widely used. HepG2 cells originated from an American patient[3], while Huh-7 were isolated from a Japanese patient[4], both affected by well-differentiated hepatocellular carcinoma. Even though these cell lines exhibit several hepatic functions, low expression of enzymes and cytochromes limit their use for metabolism and toxicity studies[5].

To study the metabolism, toxicology, and regeneration/differentiation processes, the HepaRG cell line was used as a replacement for primary hepatocytes, HepG2, and Huh-7 cells[6-8]. Isolated from an Edmonson grade I differentiated liver tumor, HepaRG cells exhibit a hepatocyte-like morphology and express hepatocyte-specific functions in defined culture conditions[9]. Nevertheless, HepaRG cells display features

of human oval ductular bipotent hepatic progenitors at confluence[10,11]. Supplementation of dimethyl sulfoxide (DMSO) to confluent HepaRG cells triggers differentiation toward hepatocytes[10,12]. Thus, the behavior of HepaRG cells is exclusive; these cells can be cultured for several passages to proliferate, or stimulated to differentiate towards fully functional hepatocyte-like cells[13].

Cellular senescence consists of a steady cell cycle block occurring because of different harmful events, which include DNA damage, oxidative stress, or even replication[14]. Stem/progenitor cells undergoing senescence cause impairment of tissue homeostasis and regeneration, caused by defective stemness and differentiation processes[15]. The induction of senescence in both HepG2 and Huh-7 cells is associated with altered gene signature, which includes changes in cell cycle regulation, signal transduction, and metabolism[16,17]. Nevertheless, to the best of our knowledge, the impact of senescence on HepaRG cells has not yet been investigated.

Thus, this study investigated whether a replication protocol would induce senescence in HepaRG cells. In addition, we characterized the effects of senescence on the transdifferentiation capacity and mitochondrial metabolism.

MATERIALS AND METHODS

Cell line and culture

The human cell line HepaRG was purchased by Merck Millipore (MMHPR116; Merck KGaA, Darmstadt, Germany). Undifferentiated HepaRG cells exhibit a fibroblast-like morphology, and the differentiation process induces both hepatocyte- and biliary-like epithelial phenotypes at confluence, indicating bipotent progenitor features[11,18]. HepaRG cells were seeded at 27000 cell/cm^2 confluence in a base medium composed by William's E Medium + GlutaMAX (3255-020; Thermo Fisher Scientific, Waltham, MA, United States) supplemented with 10% fetal bovine serum (F7524; Merck KGaA), 100 U/mL penicillin (13752; Merck KGaA), and 100 μg/mL streptomycin (P4333; Merck KGaA). Medium was changed twice a week and cells were passaged once every 7 d. Cells in passage 10 (P10, young cells) and P20 (senescent cells) were used for assays and compared. To obtain HepaRG differentiation, a two-step procedure was used as previously described. Cells were cultured in the medium for 2 wk and then in the presence of 2% DMSO for an additional 2 wk[11].

Senescence-associated β-galactosidase activity assay

The senescence-associated (SA) β-galactosidase (SA-β-gal) activity assay was performed according to the manufacturer's protocol (#9860; Cell Signaling Technology, Inc. Danvers, MA, United States). Briefly, P10 and P20 HepaRG cells grown on 6-well plates were fixed in 1X fixative solution containing 2% formaldehyde and 2% glutaraldehyde for 10 min, and then stained overnight at 37°C with the β-galactosidase staining solution at pH 6.0 for 15 h. Images were acquired using the Nikon Eclipse Ni-U microscope (Nikon, Tokyo, Japan).

Comet assay

The comet assay was performed as previously described[19]. DNA was stained with SYBR green (172-5271; Bio-Rad Laboratories, Hercules, CA, United States) just before blind slide scoring with the Nikon Eclipse Ni-U fluorescence microscope equipped with the CCD-200E video camera. At least 100 cells per sample were analyzed using the Comet Assay IV analysis software (Perceptive Instruments, Haverhill, Suffolk, United Kingdom). The extent of DNA damage in single cells was evaluated by the percentage of tail DNA.

Confocal microscopy and flow cytometry

Cells (1.5 × 10^5 cells/well) were seeded on a glass coverslip in a 24-multiwell plate. The next day, cells were washed three times with phosphate-buffered saline (PBS), fixed in 4% paraformaldehyde for 10 min at room temperature (RT), and washed twice with PBS. Cells were first permeabilized with PBS + 0.1% X-100 Triton (93418; Merck KGaA) for 10 min, and then incubated in blocking buffer (3% bovine serum albumin, A7906; Merck KGaA) + 0.3 M glycine (G-7126-500-50; Merck KGaA) for 30 min at RT. Subsequently, cells were treated for 1.5 h in the dark at RT with the following labeled antibodies: anti-cluster of differentiation 49a (CD49a) (130-101-397), anti-CD49f (130-097-246), anti-CD184 (130-098-354), anti-epithelial cell adhesion molecule (EpCAM) (130-091-253), and anti-cytokeratin 19 (CK19; 130-080-101). All antibodies were

purchased by Miltenyi Biotec B.V. & Co. KG (Bergisch Gladbach, North Rhine-Westphalia, Germany), and labeled with phycoerythrin, except anti-CK19, which was labeled with fluorescein isothiocyanate. Nuclei were counterstained with 4',6-diamidino-2-phenylindole included in mounting medium (ab104139; Abcam plc, Cambridge, United Kingdom). Cells were analyzed using the Nikon Eclipse Ti-E confocal microscope and by flow cytometry analysis using the FlowSight Cytometer (Amnis; Merck Millipore) and the IDEAS software.

Gene expression analysis

To study the levels of genes expressed in P10 and P20 HepaRG cells after differentiation, RNA was extracted from 1.0 × 10^6 cells/sample and converted into cDNA, which was used as a template in the following RT-PCR. RNA extraction was performed by the "Pure Link RNA Mini Kit" (12183025; Thermo Fisher Scientific), according to the manufacturer's protocol. RNA concentration was determined by spectrophotometer method at Nanodrop, measuring absorbance at λ = 260 nm. A260/A280 > 2 was evaluated to guarantee protein-free samples. Reverse transcription was performed using the High-Capacity cDNA Reverse Transcription Kit (4368814; Thermo Fisher Scientific), and SYBR Green (172-5271; Bio-Rad Laboratories, Hercules, CA, United States) was used as a fluorescent probe. The sequences of the forward and reverse primers for all of the genes studied are provided in Table 1.

Albumin secretion analyses

To assess the secretion of human albumin, supernatants of P10 and P20 HepaRG cells in basal conditions and after DMSO treatment were collected after 24 h of culture and assessed using a Human Albumin ELISA Kit, according to the manufacturer's instructions (ab108788; Abcam, Cambridge, United Kingdom).

CYP3A4 and γ-glutamyl transpeptidase activities

P10 and P20 HepaRG cells in basal conditions and after DMSO treatment were washed with 1× PBS, and 50 µL of 3 µM P450-Glo™ substrate (V8801; Promega, Waldorf, Germany) was added and incubated for 1 h at 37°C, 5% CO_2. Then, 25 µL substrate medium was transferred to a 96-white plate, and CYP3A4 activity was measured according to the manufacturer's protocol. HepaRG cells were homogenized in 200 µL ice-cold γ-glutamyl transpeptidase (γ-GT) assay buffer, and the γ-GT Activity Colorimetric Assay Kit (MAK089; Merck KGaA) was used according to the manufacturer's protocol.

Cell respirometry

HepaRG cells (5.0 × 10^6 cells) were washed with PBS and resuspended in 10 mmol/L KH_2PO_4, 27 mmol/L KCl, 1 mmol/L $MgCl_2$, 40 mmol/L HEPES, 0.5 mmol/L EGTA buffer (pH 7.1), and assayed for oxygen consumption by the Oxygraph Plus System (Hansatech Instruments, Norfolk, UK) at 37°C under continuous stirring. Oligomycin (8 µg/mL) was added followed the addition of valinomycin (2 µg/mL) after 5 min. The rates of oxygen consumption were corrected for 3 mmol/L potassium cyanide (KCN)-insensitive respiration and normalized to the cell number. Each experiment was repeated in triplicate.

Intracellular ATP content

Total intracellular ATP was quantified using the ENLITEN® ATP Assay System (FF2000; Promega Corporation, Madison, WI, United States), according to the manufacturer's instructions. This assay is based on luciferase, and used as the catalyzing enzyme of the ATP reaction with d-Luciferin. ATP extraction is carried out with trichloroacetic acid reagent, which releases ATP from cells, preventing its enzymatic degradation. After addition of the enzyme reagent to the intracellular extract, light emission was detected by a luminometer at 560 nm (DTX 880 Microplate Reader; Beckman Coulter, Brea, CA, United States).

Intracellular NAD^+/NADH content

Total intracellular NAD^+/NADH was quantified using the NAD/NADH-Glo Bioluminescent Assay Kit (G9072; Promega Corporation, United States), according to the manufacturer's instructions. HepaRG cells were first lysed with dodecyl trimethyl ammonium bromide and treated to neutralize their counterparts. To measure NAD^+, the extract was treated with 25 µL of 0.4 N HCl and heated at 60°C for 15 min, incubated at RT for 10 min, following the addition of 25 µL Trizma base. To quantify NADH, the extract was incubated at 60°C for 15 min followed by further incubation

Table 1 Sequences of forward and reverse primers of the genes studied

Actin	Human	FOR	5′-TGGACATCCGCAAAGACCTG-3′
		REV	5′-GCCGATCCACACGGAGTACTT-3′
Albumin	Human	FOR	5′-CCTGTTGCCAAAGCTCGATG-3′
		REV	5′-GAAATCTCTGGCTCAGGCGA-3′
CYP3A4	Human	FOR	5′-CTTCATCCAATGGACTGCATAAAT-3′
		REV	5′-TCCCAAGTATAACACTCTACACAG-3′
CEA	Human	FOR	5′-GGTCTTCAACCCAATCAGTAAGAAC-3′
		REV	5′-ATGGCCCCAGGTGAGAGG-3′
γ-GT	Human	FOR	5′-TTTGGTGTGCTGCTGGATGAC-3′
		REV	5′-ACCTGAGCTTCCCCACCTATG-3′

CEA: Carcinoembryonic antigen; CYP3A4: Cytochrome P350 3A4; FOR: Forward; γ-GT: Gamma-glutamyl transpeptidase; REV: Reverse.

for 10 min at RT. Then 50 mL HCl/Trizma solution was added to the extract. In the presence of each species, a reductase reduced a pro-luciferin reductase to luciferin. The intensity of light (proportional to the amount of each metabolite) was detected by a luminometer (DTX 880 Microplate Reader; Beckman Coulter).

Statistical analyses

Data are expressed as the mean ± standard deviation of three different experiments. Within-group variability was analyzed using Levene's test for homogeneity of variances. Differences between two groups (P10 *vs* P20) were determined by the Student's *t*-test, while two-way analysis of variance was used to test the main effects of senescence (S, P10 *vs* P20) or transdifferentiation (T, Basal *vs* DMSO) as between-subject factors; the interaction S × T was studied, and a Tukey's test was used as a post hoc test for multiple comparisons. Statistical significance was accepted when $P < 0.05$. GraphPad Prism 6.0 software was used to perform the analyses.

RESULTS

Replication induces the expression of senescence markers in HepaRG cells

Replication-induced senescence was first described in human fibroblasts because of serial culture passages[20]. Since increased SA-β-gal activity is a well-recognized marker of senescence[21], positive SA-β-gal-stained cells were counted to validate senescence in HepaRG passaged up to P10 compared to cells passaged up to P20. As shown in Figure 1A and B, replication-induced senescence in P20 HepaRG cells resulted in increased numbers of cells positive for SA-β-gal staining compared with P10 cells. A further marker of senescence is represented by the extent of DNA damage [22], determined by the comet assay, which measures the prevalence of single- and double-strand breaks. The level of DNA damage was calculated from the percentage of DNA in the tail of the comet formed after single-cell gel electrophoresis, as broken DNA moves faster in the current. The percentage of DNA in the tails *vs* the core was analyzed using Comet Assay IV software, and the results showed that P20 HepaRG cells presented with higher levels of damaged DNA than P10 cells (Figure 1C and D).

Transdifferentiation towards bipotent progenitors is altered in senescent HepaRG cells

HepaRG cells are able to actively proliferate and commit toward hepatocyte and biliary differentiation pathway, reaching maximum cell differentiation after a 2-wk DMSO exposure[11]. Then we exposed P10 and P20 HepaRG cells to DMSO, and studied the expression of markers of both progenitor and differentiated cells.

The expression of adhesion molecules such as CD49a (limited to hepatocyte-like cells) and CD49f (associated with biliary-like cells) after the differentiation process induced by DMSO was lower in P20 than in P10 HepaRG cells. Even CD184/C-X-C motif chemokine receptor 4, a known definitive endoderm marker, was less expressed

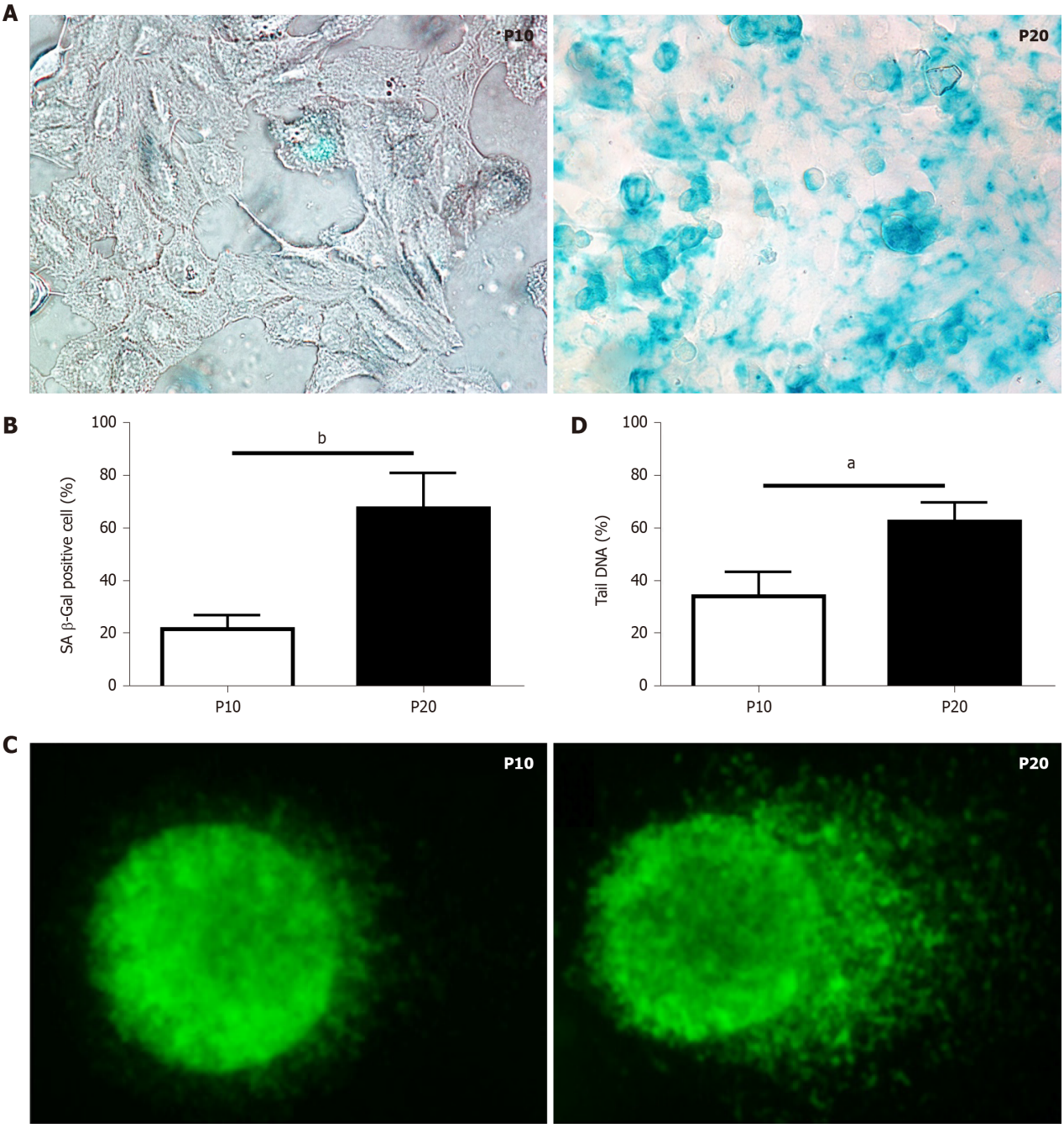

Figure 1 Characterization of markers of cellular senescence in HepaRG cells. A: Senescence-associated β-galactosidase staining of HepaRG cells at passage 10 (P10) or P20. After staining, the cells were imaged by phase contrast microscopy. Micrographs are shown at magnification 200 ×; B: Quantitative analysis of positive β-galactosidase-stained cells in P10 and P20 HepaRG cells; C: Representative images of DNA damage analysis by the comet assay in P10 and P20 HepaRG cells. After staining, the cells were imaged by fluorescence microscopy. Micrographs are shown at magnification 600 ×; D: Quantitative analysis of DNA tails from 100 cells. Data in the graphs are represented as the mean ± SD of three independent experiments. Statistical differences were assessed by the Student's *t*-test. [a]*P* < 0.05 *vs* P10; [b]*P* < 0.01 *vs* P10.

in P20 than in P10 HepaRG cells exposed to DMSO. Moreover, the differentiation protocol resulted in lower expression of EpCAM and CK19 (markers of hepatic progenitor cells[23]) in P20 than in P10 HepaRG cells (Figures 2 and 3).

The expression of genes typical of a differentiated status, such as albumin, CYP3A4 and γ-GT, and of CEA as marker of undifferentiation was next determined in HepaRG cells before and after DMSO exposure. The results obtained by statistical analyses aimed to test the main effects of S, of T, and the interaction S × T. The main effect of S was significant for the expression of all the genes studied (albumin: $F_{(1,8)}$ = 44.54, *P* = 0.0002; CYP3A4: $F_{(1,8)}$ = 24.22, *P* = 0.0012; γ-GT: $F_{(1,8)}$ = 46.82, *P* = 0.0001; CEA: $F_{(1,8)}$ = 12.24, *P* = 0.0081). The main effect of T was significant for the expression of albumin ($F_{(1,8)}$ = 243.3, *P* < 0.0001), CYP3A4 ($F_{(1,8)}$ = 37.50, *P* = 0.0003), and γ-GT ($F_{(1,8)}$ = 190.2, *P* < 0.0001), but not for CEA. The interaction between S and T was significant for the

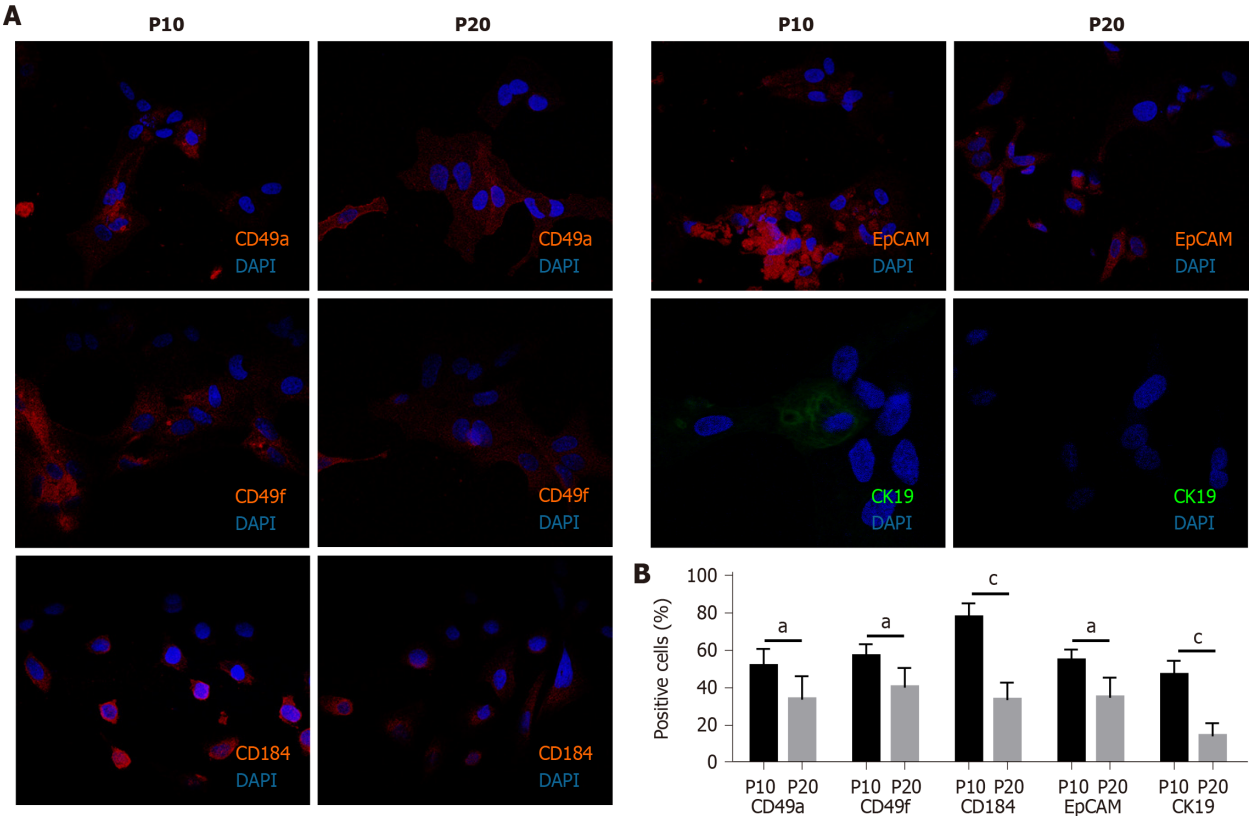

Figure 2 Expression of progenitor markers in HepaRG cells after the transdifferentiation process. A: Representative immunofluorescence images of HepaRG cells at passage 10 (P10) or P20. After staining, the cells were imaged by confocal microscopy. Micrographs are shown at magnification 200 ×; B: Quantitative analysis of positively stained cells in P10 and P20 HepaRG cells. Data in the graphs are represented as the mean ± standard deviation of three independent experiments. Statistical differences were assessed by the Student's *t*-test. $^{a}P < 0.05$ *vs* P10; $^{c}P < 0.001$ *vs* P10.

expression of all the genes studied (albumin: $F_{(1,8)} = 43.95$, $P = 0.0002$; CYP3A4: $F_{(1,8)} = 24.22$, $P = 0.0012$; γ-GT: $F_{(1,8)} = 60.71$, $P < 0.0001$; CEA: $F_{(1,8)} = 10.13$, $P = 0.0129$). Post hoc analysis showed that the expression of albumin, CYP3A4 and γ-GT was induced by DMSO exposure both in P10 and in P20 HepaRG cells, supporting the transdifferentiation process; however, mRNA levels were lower in DMSO-treated P20 rather than P10 HepaRG cells (Figure 4A-C). Finally, the expression of CEA was reduced by DMSO exposure in P10 but not in P20 HepaRG cells (Figure 4D).

The same analysis was performed on specific functional activities of HepaRG cells, studying albumin secretion, CYP3A4 and γ-GT activity, and the results are represented in Figure 5. In particular, we found a main effect of S (albumin secretion: $F_{(1,8)} = 20.95$, $P = 0.0018$; CYP3A4 activity: $F_{(1,8)} = 10.24$, $P = 0.0126$; γ-GT activity: $F_{(1,8)} = 18.13$, $P = 0.0028$), T (albumin secretion: $F_{(1,8)} = 120.2$, $P < 0.0001$, CYP3A4 activity: $F_{(1,8)} = 9.15$, $P = 0.0164$; γ-GT activity: $F_{(1,8)} = 68.25$, $P < 0.0001$), and interaction between S and T (albumin secretion: $F_{(1,8)} = 20.53$, $P = 0.0019$; CYP3A4 activity: $F_{(1,8)} = 7.181$, $P = 0.0233$; γ-GT activity: $F_{(1,8)} = 19.36$, $P = 0.0023$). Post hoc analysis showed that albumin secretion, CYP3A4 and γ-GT activities were reduced in DMSO-treated P20 rather than P10 HepaRG cells.

Taken together, these results suggest that the transdifferentiation process triggered by DMSO in HepaRG cells is hampered by the replication-induced senescence.

Senescence-induced impairment of HepaRG transdifferentiation is associated with mitochondrial dysfunction

Mitochondrial dysfunction is recognized as one of the hallmarks of senescence[24]. Thus, we performed respirometry analyses in HepaRG by high-resolution oximetry. Figure 6A details the protocol used and is representative of the oxygraphic profiles in young (P10) and senescent (P20) HepaRG cells in basal conditions and after the transdifferentiation protocol (DMSO). The resting respiration (RR), which depends on endogenous substrates, was impacted by both the S and the T factor (S: $F_{(1,8)} = 78.38$, $P < 0.0001$; T: $F_{(1,8)} = 57.12$, $P < 0.0001$), and by the interaction S×T ($F_{(1,8)} = 60.86$, $P < 0.0001$). Addition of oligomycin (a F_oF_1-ATP synthase inhibitor) reduced the oxygen uptake, suggesting that most of the mitochondrial respiration was coupled to the

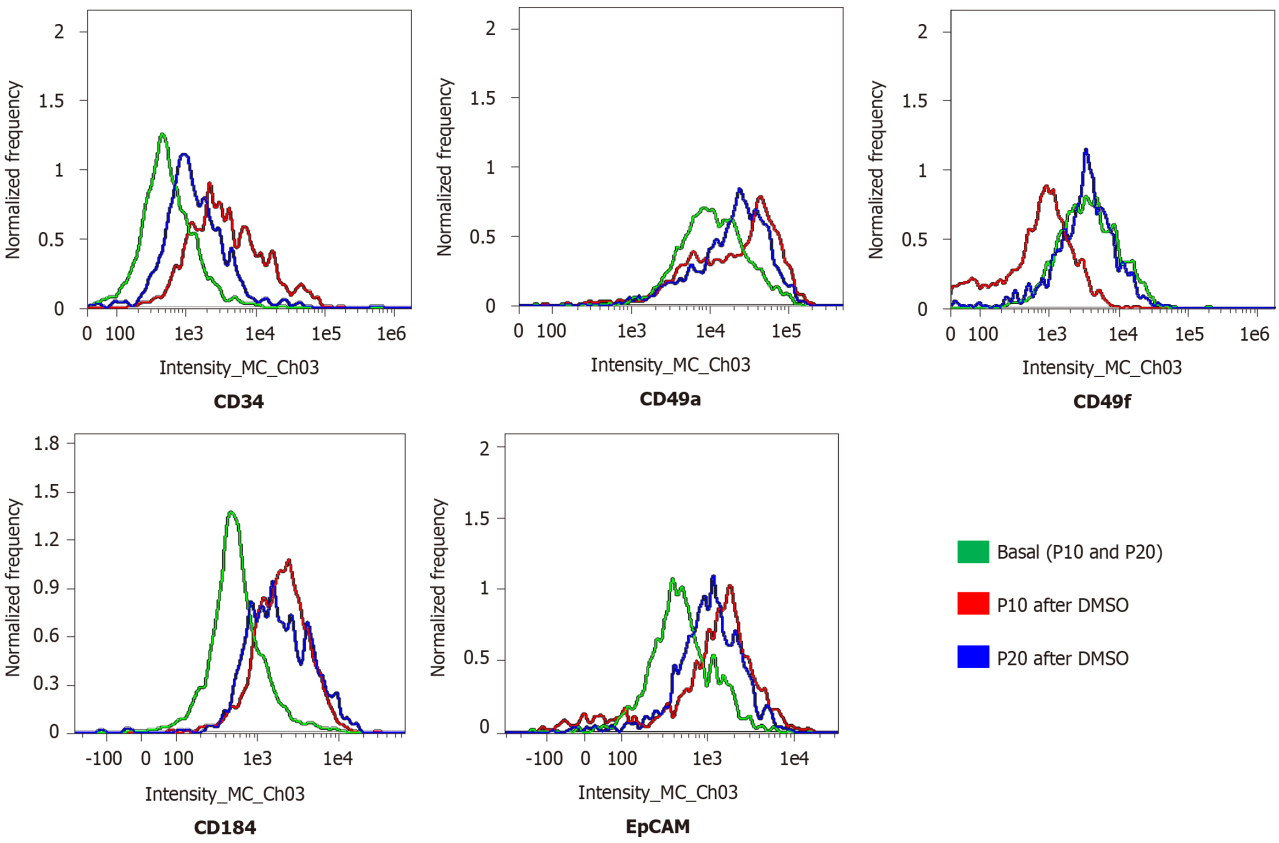

Figure 3 Expression of progenitor markers in HepaRG cells before and after the transdifferentiation process. Flow cytometry histograms of HepaRG cells at passage 10 (P10) or P20 in basal conditions or after the transdifferentiation protocol (dimethyl sulfoxide). After staining, the cells were analyzed with flow cytometry.

synthesis of ATP. Nevertheless, both the S and the T factor impacted this parameter (S: $F_{(1,8)}$ = 10.83, P = 0.0018; T: $F_{(1,8)}$ = 6.847, P = 0.0308), as well as the interaction S × T ($F_{(1,8)}$ = 8.104, P = 0.0216). Restoration of the oxygen uptake by the addition of valinomycin (a K^+ ionophore which uncouples oxygen consumption from ATP synthesis) was also impacted by both the S and the T factor (S: $F_{(1,8)}$ = 59.58, P < 0.0001; T: $F_{(1,8)}$ = 53.09, P < 0.0001), and the interaction S × T ($F_{(1,8)}$ = 55.97, P < 0.0001). The post hoc analysis showed that the oxygen uptake in all the examined conditions was higher in P10 HepaRG cells after the transdifferentiation protocol with respect to the other samples (Figure 6B). The effects of both S and T, and their interaction, was observed on the ATP-dependent oxygen uptake, calculated as the difference between RR and oligomycin-induced respiration (S: $F_{(1,8)}$ = 28.94, P = 0.0007; T: $F_{(1,8)}$ = 25.35, P = 0.001; S × T: $F_{(1,8)}$ = 27.36, P = 0.0008). The post hoc analysis showed that the P10 HepaRG cells after the transdifferentiation protocol exhibited a higher ATP-dependent oxygen uptake than the other samples (Figure 6C). The respiratory control ratio (RCR), calculated as the ratio between RR and oligomycin-induced respiration, was also influenced by both S and T (S: $F_{(1,8)}$ = 14.76, P = 0.0049; T: $F_{(1,8)}$ = 13.43, P = 0.0064), and their interaction (S × T: $F_{(1,8)}$ = 11.38, P = 0.0097). The post hoc analysis resulted in a higher RCR for the P10 HepaRG cells after the transdifferentiation protocol compared to the other samples (Figure 6D). Taken together, these data suggest that the transdifferentiation induced by DMSO increases mitochondrial respiration in HepaRG cells; however, this does not occur in senescent cells.

To confirm a defect in mitochondrial dysfunction of senescent HepaRG, the cellular ATP concentration was further measured. We observed a significant effect of both S and T (S:$F_{(1,8)}$ = 14.89, P = 0.0048; T:$F_{(1,8)}$ = 12.15, P = 0.0083), and the post hoc analysis showed that the ATP content of transdifferentiated P10 HepaRG cells was higher than the other samples (Figure 7A). SA mitochondrial dysfunction can be consequent to an exhaustion of the oxidized form of NAD^+[25]. The analysis of NAD^+/NADH content in HepaRG cells revealed no changes in NADH; nevertheless, the impact of S, T, and their interaction was observed on both NAD^+ (S:$F_{(1,8)}$ = 13.84, P = 0.0059; T:$F_{(1,8)}$ = 26.00, P = 0.0009; S × T: $F_{(1,8)}$ = 10.47, P = 0.0120) and NAD^+/NADH (S:$F_{(1,8)}$ = 22.23, P = 0.0015; T:$F_{(1,8)}$ = 19.75, P = 0.0022; S × T: $F_{(1,8)}$ = 10.02, P = 0.0133). The post hoc analysis resulted

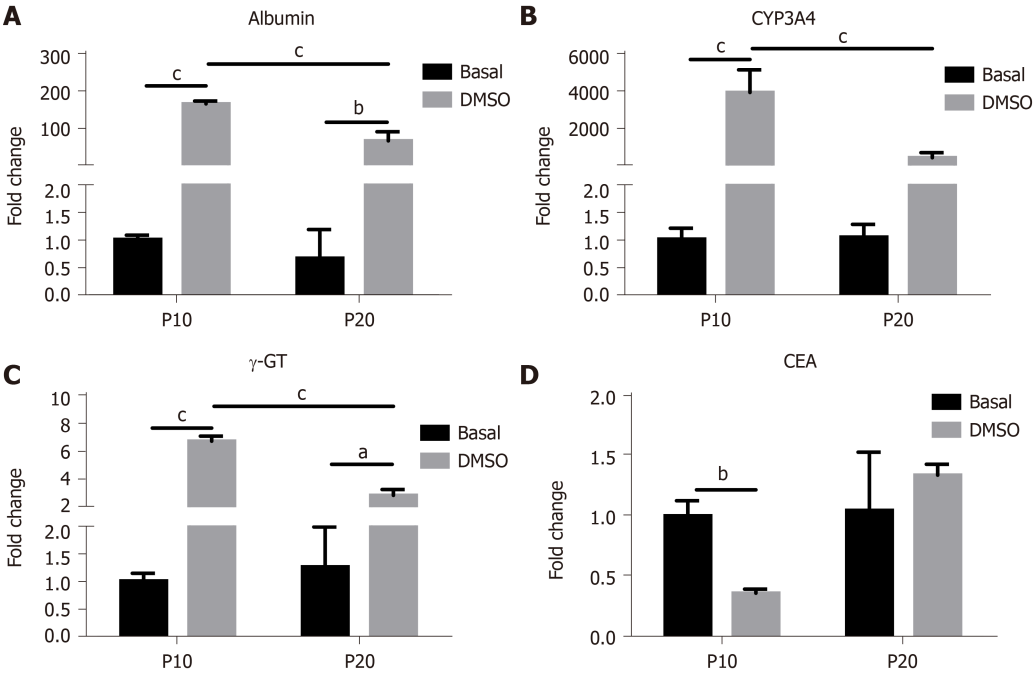

Figure 4 Gene expression analysis in HepaRG cells at passage 10 or passage 20 in basal conditions or after the transdifferentiation protocol (dimethyl sulfoxide). A: mRNA level of albumin; B: Cytochrome P350 3A4 (CYP3A4); C: Gamma-glutamyl transpeptidase (γ-GT); D: Carcinoembryonic antigen (CEA) measured by reverse transcription-polymerase chain reaction. Data in the graphs are represented as the mean ± standard deviation of three independent experiments. Statistical differences were assessed by two-way analysis of variance followed by the Tukey test as the post hoc test. $^{a}P < 0.05$; $^{b}P < 0.01$; $^{c}P < 0.001$. P10: Passage 10; P20: Passage 20; DMSO: Dimethyl sulfoxide.

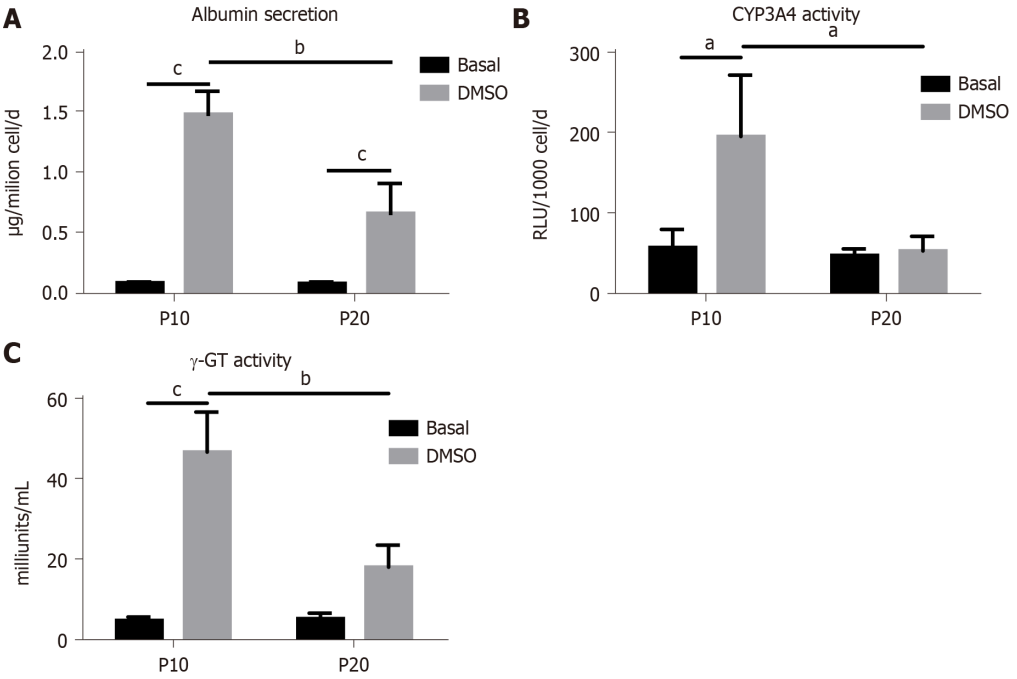

Figure 5 Functional tests in HepaRG cells at passage 10 or passage 20) in basal conditions or after the transdifferentiation protocol (dimethyl sulfoxide). A: Albumin secretion; B: Cytochrome P350 3A4 (CYP3A4); C: Gamma-glutamyl transpeptidase (γ-GT) activities. Data in the graphs are represented as the mean ± standard deviation of three independent experiments. Statistical differences were assessed by two-way analysis of variance followed by the Tukey test as the post hoc test. $^{a}P < 0.05$; $^{b}P < 0.01$; $^{c}P < 0.001$. P10: Passage 10; P20: Passage 20; DMSO: Dimethyl sulfoxide.

in higher NAD^+ and NAD^+/NADH in transdifferentiated P10 HepaRG cells with respect to the other samples (Figure 7B).

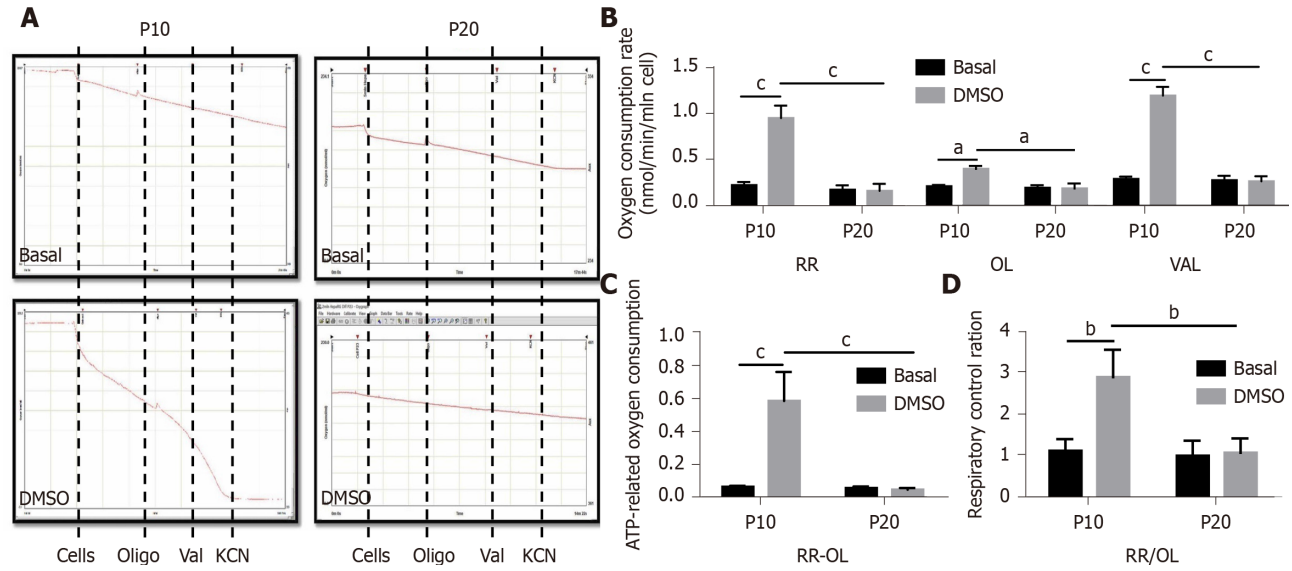

Figure 6 Measurement of mitochondrial respiration in HepaRG cells at passage 10 or passage 20 in basal conditions or after the transdifferentiation protocol (dimethyl sulfoxide). A: Representative oxymetric traces of mitochondrial respiration in HepaRG cells. Where indicated, the following were added: 4 × 10^6 HepaRG cells, 8 μg/mL oligomycin (OL), 2 μg/mL valinomycin (VAL), 3 mmol/L potassium cyanide (KCN). The continuous line represents the oxygen concentration measured every 0.1 s throughout the time-course of the assay; B: Representative graph of the normalized and KCN-insensitive-corrected oxygen consumption rates measured under resting respiration (RR) conditions, in the presence of OL and in the presence of VAL (see panel A); C: ATP-dependent oxygen consumption measured as absolute difference between that obtained in the absence and that in the presence of oligomycin (RR-OL); D: Respiratory control ratios obtained dividing the oxygen consumption rates measured under resting conditions by that in the presence of oligomycin (RR/OL). Data in the graphs are represented as the mean ± standard deviation of three independent experiments. Statistical differences were assessed by two-way analysis of variance followed by the Tukey's test as the post hoc test. [a]$P < 0.05$; [b]$P < 0.01$; [c]$P < 0.001$. DMSO: Dimethyl sulfoxide; P10: Passage 10; P20: Passage 20.

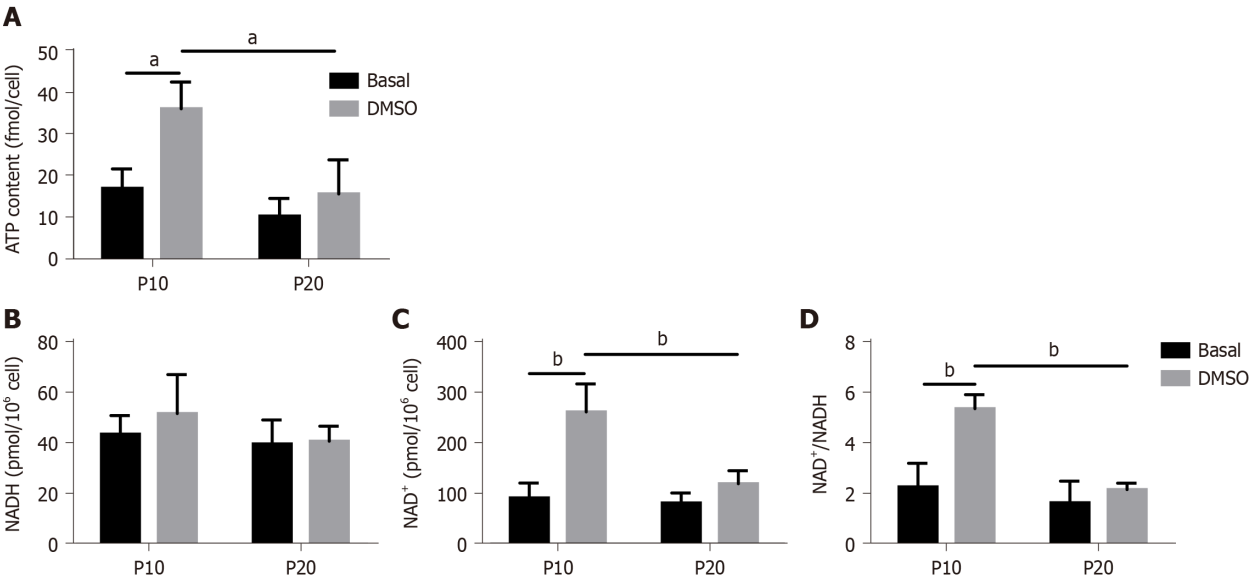

Figure 7 ATP and nicotinamide adenine dinucleotide (NAD)/NAD with hydrogen content in HepaRG cells at passage 10 or passage 20 in basal conditions or after the transdifferentiation protocol (dimethyl sulfoxide). A: Cellular ATP content was expressed as ATP concentration/cells; B: Intracellular nicotinamide adenine dinucleotide (NAD^+) and NAD with hydrogen (NADH) were extracted, and NAD^+ and NADH levels were measured using a microplate reader. NAD^+/NADH ratio was calculated based on the concentration of NAD^+ and NADH. Data in the graphs are represented as the mean ± standard deviation of three independent experiments. Statistical differences were assessed by two-way analysis of variance followed by the Tukey's test as the post hoc test. [a]$P < 0.05$; [b]$P < 0.01$. DMSO: Dimethyl sulfoxide; P10: Passage 10; P20: Passage 20.

DISCUSSION

This study demonstrates that cellular replication in HepaRG cells is associated with both the expression of senescence markers and the reduction in transdifferentiation potential. Indeed, data related to phenotype, gene expression, functional analysis, and

mitochondrial function suggest that the transdifferentiation process of HepaRG is preserved after a few passages, but it is altered by continuous replication.

HepaRG represents a unique cell line characterized by high expression of detoxifying and metabolizing enzymes, transport proteins, and nuclear receptors, as well as the ability to transdifferentiate toward hepatocyte-like and cholangiocyte-like cells[9-11]. Other than representing a viable tool for cell biology, drug metabolism, and virology studies, differentiated HepaRG cells are suitable to generate humanized liver in rodent models, allowing *in vivo* studies of liver development and physiology[26,27].

Cultured cells stop proliferating after a finite number of divisions, a phenomenon defined to as replicative senescence[28,29]. However, cells can escape replicative senescence by several mechanisms, including overexpression of viral genes such as simian virus 40 large T antigen (which inactivates p53), or telomerase reverse transcriptase protein (TERT, which elongates telomeres)[30,31]. Proliferating HepaRG cells show over-expression and hyper-activation of human TERT, as well as inhibition of p21 and p27, which in turn inhibit the catalytic activity of cyclin-dependent kinases and stop the cell cycle[32]. Nevertheless, our data demonstrate that a replication protocol induces the expression of senescence markers in HepaRG cells, such as positive SA-β-gal staining and DNA alterations. Thus, we hypothesize that the mechanisms that induce senescence in HepaRG cells are different from telomere shortening and p21/p27 activation.

Senescence impairs the transdifferentiation of several cell lines[33-36]. Senescent cells secrete a large variety of molecules that change the surrounding microenvironment, with consequent alterations of differentiation and tissue regeneration[37,38]. These compounds include a wide range of cytokines, growth factors, and signaling molecules that are included in the SA secretory phenotype (SASP)[39]. Our data clearly demonstrate that replicative senescence alters the transdifferentiation process of HepaRG cells. Nevertheless, we did not analyze the SASP in our study, since this marker is strictly linked with telomere shortening[40]. By contrast, we focused on mitochondria, since the homeostasis of these organelles is crucial for several aspects of senescence including SASP[41]. Indeed, the impairment of mitochondrial oxidative phosphorylation (OxPhos) is mainly involved in the early steps of cell senescence[42]. Moreover, senescent cells exhibit severe metabolic alterations associated with mitochondrial metabolites, such as oxidized to reduced NAD ratios (NAD+/NADH)[43]. The novel and straight findings of this study demonstrate the higher mitochondria-related respiration in transdifferentiated HepaRG cells, which was not observed after induction of replicative senescence. Indeed, this respiration was suppressed by oligomycin, a specific inhibitor of ATP synthase, suggesting that transdifferentiated HepaRG cells in resting conditions oxidize substrates to synthetize ATP through the OxPhos system. On the other hand, senescent HepaRG cells subjected to the transdifferentiation protocol exhibited lower oxygen consumption which was insensitive to oligomycin. These results are consistent with a transition from a glycolytic to an oxidative metabolism in transdifferentiated HepaRG cells, which did not occur in senescent cells. Of interest, the RR in transdifferentiated HepaRG cells was lower than that reached in the presence of an uncoupler (maximal respiratory rate), indicating the existence of a respiratory reserve. By contrast, the RR of senescent HepaRG cells undergoing transdifferentiation was similar to the maximal respiratory rate, suggesting the absence of a respiratory reserve. Mitochondrial dysfunction in senescent HepaRG cells after transdifferentiation was further confirmed by a reduction in cellular ATP concentration.

The concentration of the oxidized form of NAD^+ is determinant for mitochondrial homeostasis[44,45]. Moreover, NAD^+ is crucial in several metabolic pathways, including glycolysis, citric acid cycle, and OxPhos, with consequent implications for both stemness/differentiation and cell senescence[46]. Cells that maintain a physiological quiescent state to preserve long-term self-renewal capacity are characterized by low NAD^+ levels to obtain energy from glycolysis; on the contrary, cell differentiation leads to reduced glycolysis and increased OhPhos, which require high NAD^+ levels[47]. Age-related reductions of both NAD^+ levels and NAD^+/NADH ratio are evolutionarily preserved, and consistent evidence for low NAD^+ has been provided for several old mammalian tissues[48]. Our data show that HepaRG transdifferentiation is associated with increased NAD^+ and relatively stable NADH, with consequent high NAD^+/NADH. However, the raise of both NAD^+ and NAD^+/NADH is not observed in HepaRG undergoing replicative senescence. Even though the effect of a treatment goes beyond the scope of our study, it is conceivable that a replenishment of NAD^+ would protect mitochondria and improve the transdifferentiation process of senescent HepaRG cells, as already described for other cell types[49-51].

CONCLUSION

In conclusion, the present report demonstrates that HepaRG cells undergo replicative senescence, which is associated with impairment in transdifferentiation, mitochondrial dysfunction, and NAD^+ depletion. Further investigations are required to refine the molecular mechanism underlying such observation. The limitations in the transdifferentiation potential of senescent HepaRG cells, with consequent alteration of metabolic and regenerative properties, may have serious implications when this cell line is applied for basic studies.

ARTICLE HIGHLIGHTS

Research background

The HepaRG cell line is used to study metabolism, toxicology, and the regeneration/differentiation processes, as a replacement to primary hepatocytes, HepG2, and Huh-7 cells. These cells exhibit a hepatocyte-like morphology and express hepatocyte-specific functions in defined culture conditions; furthermore, HepaRG display features of human oval ductular bipotent hepatic progenitors.

Research motivation

Cellular senescence consists in a steady cell cycle block occurring because of different harmful events, leading to defective stemness and differentiation processes, as well as changes in cell cycle regulation, signal transduction, and metabolism. The impact of senescence on HepaRG cells has not yet been investigated.

Research objectives

This study investigated whether a replication protocol would induce senescence in HepaRG cells. In addition, we characterized the effects of senescence on transdifferentiation capacity and mitochondrial metabolism.

Research methods

The transdifferentiation capacity of HepaRG cells over passage 10 (P10) *vs* passage 20 (P20) was compared. To stimulate transdifferentiation, HepaRG cells were treated with dimethyl sulfoxide (DMSO). Aging was evaluated by senescence-associated (SA) β-galactosidase activity and the comet assay. HepaRG transdifferentiation was analyzed by confocal microscopy and flow cytometry (expression of cluster of differentiation 49a [CD49a], CD49f, CD184, epithelial cell adhesion molecule [EpCAM], and cytokeratin 19 [CK19]), by quantitative PCR analysis (expression of albumin, cytochrome P450 3A4 [CYP3A4], γ-glutamyl transpeptidase [γ-GT] and carcinoembryonic antigen [CEA]) and functional analysis (albumin secretion, CYP3A4 and γ-GT). Mitochondrial respiration, the ATP and the NAD^+/NADH content were also measured.

Research results

We first observed that replication induces the expression of senescence markers in HepaRG cells, since SA β-galactosidase staining was higher in P20 than in P10 HepaRG cells, and the comet assay showed a consistent DNA damage in P20 HepaRG cells. We further reported that transdifferentiation towards bipotent progenitors is altered in senescent HepaRG cells, as P20 HepaRG cells exhibited a reduction of CD49a, CD49f, CD184, EpCAM and CK19 – with respect to P10 – after DMSO treatment. Furthermore, the lower gene expression of albumin, CYP3A4, and γ-GT, as well as the reduced albumin secretion capacity, CYP3A4, and γ-GT activity were reported in transdifferentiated P20 compared to P10 cells. By contrast, the gene expression level of CEA was not reduced by transdifferentiation in P20 cells. Finally, we show that senescence-induced impairment of HepaRG transdifferentiation is associated with mitochondrial dysfunction, since both cellular and mitochondrial oxygen consumption were lower in P20 than in P10 transdifferentiated cells, and both ATP and NAD^+/NADH were depleted in P20 cells with respect to P10 cells.

Research conclusions

The present study demonstrates that HepaRG cells undergo replicative senescence, with consequent impairment in transdifferentiation, functional activity, mitochondrial dysfunction, and NAD^+ depletion.

Research perspectives

Further studies will define the molecular mechanisms underlying our observations. The limitations in the transdifferentiation potential of senescent HepaRG cells, with consequent alteration of metabolic and regenerative properties, may have serious implications when this cell line is applied for basic studies.

REFERENCES

1 **Fabre G**, Combalbert J, Berger Y, Cano JP. Human hepatocytes as a key *in vitro* model to improve preclinical drug development. *Eur J Drug Metab Pharmacokinet* 1990; **15**: 165-171 [PMID: 2200686 DOI: 10.1007/BF03190200]

2 **Madan A**, Graham RA, Carroll KM, Mudra DR, Burton LA, Krueger LA, Downey AD, Czerwinski M, Forster J, Ribadeneira MD, Gan LS, LeCluyse EL, Zech K, Robertson P Jr, Koch P, Antonian L, Wagner G, Yu L, Parkinson A. Effects of prototypical microsomal enzyme inducers on cytochrome P450 expression in cultured human hepatocytes. *Drug Metab Dispos* 2003; **31**: 421-431 [PMID: 12642468 DOI: 10.1124/dmd.31.4.421]

3 **Javitt NB**. Hep G2 cells as a resource for metabolic studies: lipoprotein, cholesterol, and bile acids. *FASEB J* 1990; **4**: 161-168 [PMID: 2153592 DOI: 10.1096/fasebj.4.2.2153592]

4 **Nakabayashi H**, Taketa K, Miyano K, Yamane T, Sato J. Growth of human hepatoma cells lines with differentiated functions in chemically defined medium. *Cancer Res* 1982; **42**: 3858-3863 [PMID: 6286115]

5 **Bulutoglu B**, Rey-Bedón C, Mert S, Tian L, Jang YY, Yarmush ML, Usta OB. A comparison of hepato-cellular *in vitro* platforms to study CYP3A4 induction. *PLoS One* 2020; **15**: e0229106 [PMID: 32106230 DOI: 10.1371/journal.pone.0229106]

6 **McGill MR**, Yan HM, Ramachandran A, Murray GJ, Rollins DE, Jaeschke H. HepaRG cells: a human model to study mechanisms of acetaminophen hepatotoxicity. *Hepatology* 2011; **53**: 974-982 [PMID: 21319200 DOI: 10.1002/hep.24132]

7 **Anthérieu S**, Chesné C, Li R, Guguen-Guillouzo C, Guillouzo A. Optimization of the HepaRG cell model for drug metabolism and toxicity studies. *Toxicol In Vitro* 2012; **26**: 1278-1285 [PMID: 22643240 DOI: 10.1016/j.tiv.2012.05.008]

8 **Dubuquoy L**, Louvet A, Lassailly G, Truant S, Boleslawski E, Artru F, Maggiotto F, Gantier E, Buob D, Leteurtre E, Cannesson A, Dharancy S, Moreno C, Pruvot FR, Bataller R, Mathurin P. Progenitor cell expansion and impaired hepatocyte regeneration in explanted livers from alcoholic hepatitis. *Gut* 2015; **64**: 1949-1960 [PMID: 25731872 DOI: 10.1136/gutjnl-2014-308410]

9 **Gripon P**, Rumin S, Urban S, Le Seyec J, Glaise D, Cannie I, Guyomard C, Lucas J, Trepo C, Guguen-Guillouzo C. Infection of a human hepatoma cell line by hepatitis B virus. *Proc Natl Acad Sci U S A* 2002; **99**: 15655-15660 [PMID: 12432097 DOI: 10.1073/pnas.232137699]

10 **Parent R**, Marion MJ, Furio L, Trépo C, Petit MA. Origin and characterization of a human bipotent liver progenitor cell line. *Gastroenterology* 2004; **126**: 1147-1156 [PMID: 15057753 DOI: 10.1053/j.gastro.2004.01.002]

11 **Cerec V**, Glaise D, Garnier D, Morosan S, Turlin B, Drenou B, Gripon P, Kremsdorf D, Guguen-Guillouzo C, Corlu A. Transdifferentiation of hepatocyte-like cells from the human hepatoma HepaRG cell line through bipotent progenitor. *Hepatology* 2007; **45**: 957-967 [PMID: 17393521 DOI: 10.1002/hep.21536]

12 **Troadec MB**, Glaise D, Lamirault G, Le Cunff M, Guérin E, Le Meur N, Détivaud L, Zindy P, Leroyer P, Guisle I, Duval H, Gripon P, Théret N, Boudjema K, Guguen-Guillouzo C, Brissot P, Léger JJ, Loréal O. Hepatocyte iron loading capacity is associated with differentiation and repression of motility in the HepaRG cell line. *Genomics* 2006; **87**: 93-103 [PMID: 16325370 DOI: 10.1016/j.ygeno.2005.08.016]

13 **Guillouzo A**, Corlu A, Aninat C, Glaise D, Morel F, Guguen-Guillouzo C. The human hepatoma HepaRG cells: a highly differentiated model for studies of liver metabolism and toxicity of xenobiotics. *Chem Biol Interact* 2007; **168**: 66-73 [PMID: 17241619 DOI: 10.1016/j.cbi.2006.12.003]

14 **Hernandez-Segura A**, Nehme J, Demaria M. Hallmarks of Cellular Senescence. *Trends Cell Biol* 2018; **28**: 436-453 [PMID: 29477613 DOI: 10.1016/j.tcb.2018.02.001]

15 **van Deursen JM**. The role of senescent cells in ageing. *Nature* 2014; **509**: 439-446 [PMID: 24848057 DOI: 10.1038/nature13193]

16 **Yildiz G**, Arslan-Ergul A, Bagislar S, Konu O, Yuzugullu H, Gursoy-Yuzugullu O, Ozturk N, Ozen C, Ozdag H, Erdal E, Karademir S, Sagol O, Mizrak D, Bozkaya H, Ilk HG, Ilk O, Bilen B, Cetin-Atalay R, Akar N, Ozturk M. Genome-wide transcriptional reorganization associated with senescence-to-immortality switch during human hepatocellular carcinogenesis. *PLoS One* 2013; **8**: e64016 [PMID: 23691139 DOI: 10.1371/journal.pone.0064016]

17 **Aravinthan A**, Challis B, Shannon N, Hoare M, Heaney J, Alexander GJM. Selective insulin resistance in hepatocyte senescence. *Exp Cell Res* 2015; **331**: 38-45 [PMID: 25263463 DOI: 10.1016/j.yexcr.2014.09.025]

18 **Aninat C**, Piton A, Glaise D, Le Charpentier T, Langouët S, Morel F, Guguen-Guillouzo C, Guillouzo A. Expression of cytochromes P450, conjugating enzymes and nuclear receptors in human hepatoma HepaRG cells. *Drug Metab Dispos* 2006; **34**: 75-83 [PMID: 16204462 DOI:

10.1124/dmd.105.006759]
19 **Jossé R**, Aninat C, Glaise D, Dumont J, Fessard V, Morel F, Poul JM, Guguen-Guillouzo C, Guillouzo A. Long-term functional stability of human HepaRG hepatocytes and use for chronic toxicity and genotoxicity studies. *Drug Metab Dispos* 2008; **36**: 1111-1118 [PMID: 18347083 DOI: 10.1124/dmd.107.019901]
20 **Hayflick L**, MOORHEAD PS. The serial cultivation of human diploid cell strains. *Exp Cell Res* 1961; **25**: 585-621 [PMID: 13905658 DOI: 10.1016/0014-4827(61)90192-6]
21 **Kurz DJ**, Decary S, Hong Y, Erusalimsky JD. Senescence-associated (beta)-galactosidase reflects an increase in lysosomal mass during replicative ageing of human endothelial cells. *J Cell Sci* 2000; **113**: 3613-3622 [PMID: 11017877]
22 **Kuilman T**, Michaloglou C, Mooi WJ, Peeper DS. The essence of senescence. *Genes Dev* 2010; **24**: 2463-2479 [PMID: 21078816 DOI: 10.1101/gad.1971610]
23 **Yovchev MI**, Grozdanov PN, Zhou H, Racherla H, Guha C, Dabeva MD. Identification of adult hepatic progenitor cells capable of repopulating injured rat liver. *Hepatology* 2008; **47**: 636-647 [PMID: 18023068 DOI: 10.1002/hep.22047]
24 **López-Otín C**, Blasco MA, Partridge L, Serrano M, Kroemer G. The hallmarks of aging. *Cell* 2013; **153**: 1194-1217 [PMID: 23746838 DOI: 10.1016/j.cell.2013.05.039]
25 **Gomes AP**, Price NL, Ling AJ, Moslehi JJ, Montgomery MK, Rajman L, White JP, Teodoro JS, Wrann CD, Hubbard BP, Mercken EM, Palmeira CM, de Cabo R, Rolo AP, Turner N, Bell EL, Sinclair DA. Declining NAD(+) induces a pseudohypoxic state disrupting nuclear-mitochondrial communication during aging. *Cell* 2013; **155**: 1624-1638 [PMID: 24360282 DOI: 10.1016/j.cell.2013.11.037]
26 **Jiang L**, Li JG, Lan L, Wang YM, Mao Q, You JP. Human hepatoma HepaRG cell line engraftment in severe combined immunodeficient × beige mice using mouse-specific anti-Fas antibody. *Transplant Proc* 2010; **42**: 3773-3778 [PMID: 21094855 DOI: 10.1016/j.transproceed.2010.08.064]
27 **Higuchi Y**, Kawai K, Yamazaki H, Nakamura M, Bree F, Guguen-Guillouzo C, Suemizu H. The human hepatic cell line HepaRG as a possible cell source for the generation of humanized liver TK-NOG mice. *Xenobiotica* 2014; **44**: 146-153 [PMID: 24066694 DOI: 10.3109/00498254.2013.836257]
28 **HAYFLICK L**. THE LIMITED IN VITRO LIFETIME OF HUMAN DIPLOID CELL STRAINS. *Exp Cell Res* 1965; **37**: 614-636 [PMID: 14315085 DOI: 10.1016/0014-4827(65)90211-9]
29 **Coates PJ**. Markers of senescence? *J Pathol* 2002; **196**: 371-373 [PMID: 11920730 DOI: 10.1002/path.1073]
30 **Bodnar AG**, Ouellette M, Frolkis M, Holt SE, Chiu CP, Morin GB, Harley CB, Shay JW, Lichtsteiner S, Wright WE. Extension of life-span by introduction of telomerase into normal human cells. *Science* 1998; **279**: 349-352 [PMID: 9454332 DOI: 10.1126/science.279.5349.349]
31 **Ali SH**, DeCaprio JA. Cellular transformation by SV40 Large T antigen: interaction with host proteins. *Semin Cancer Biol* 2001; **11**: 15-23 [PMID: 11243895 DOI: 10.1006/scbi.2000.0342]
32 **Sirma H**, Kumar M, Meena JK, Witt B, Weise JM, Lechel A, Ande S, Sakk V, Guguen-Guillouzo C, Zender L, Rudolph KL, Günes C. The promoter of human telomerase reverse transcriptase is activated during liver regeneration and hepatocyte proliferation. *Gastroenterology* 2011; **141**: 326-337, 337.e1 [PMID: 21447332 DOI: 10.1053/j.gastro.2011.03.047]
33 **Sun CK**, Zhou D, Zhang Z, He L, Zhang F, Wang X, Yuan J, Chen Q, Wu LG, Yang Q. Senescence impairs direct conversion of human somatic cells to neurons. *Nat Commun* 2014; **5**: 4112 [PMID: 24934763 DOI: 10.1038/ncomms5112]
34 **García-Prat L**, Muñoz-Cánoves P. Aging, metabolism and stem cells: Spotlight on muscle stem cells. *Mol Cell Endocrinol* 2017; **445**: 109-117 [PMID: 27531569 DOI: 10.1016/j.mce.2016.08.021]
35 **Moimas S**, Salton F, Kosmider B, Ring N, Volpe MC, Bahmed K, Braga L, Rehman M, Vodret S, Graziani ML, Wolfson MR, Marchetti N, Rogers TJ, Giacca M, Criner GJ, Zacchigna S, Confalonieri M. miR-200 family members reduce senescence and restore idiopathic pulmonary fibrosis type II alveolar epithelial cell transdifferentiation. *ERJ Open Res* 2019; **5** [PMID: 31857992 DOI: 10.1183/23120541.00138-2019]
36 **Han L**, Zhang Y, Zhang M, Guo L, Wang J, Zeng F, Xu D, Yin Z, Xu Y, Wang D, Zhou H. Interleukin-1β-Induced Senescence Promotes Osteoblastic Transition of Vascular Smooth Muscle Cells. *Kidney Blood Press Res* 2020; **45**: 314-330 [PMID: 32126555 DOI: 10.1159/000504298]
37 **Baar MP**, Perdiguero E, Muñoz-Cánoves P, de Keizer PL. Musculoskeletal senescence: a moving target ready to be eliminated. *Curr Opin Pharmacol* 2018; **40**: 147-155 [PMID: 29883814 DOI: 10.1016/j.coph.2018.05.007]
38 **Nicaise AM**, Wagstaff LJ, Willis CM, Paisie C, Chandok H, Robson P, Fossati V, Williams A, Crocker SJ. Cellular senescence in progenitor cells contributes to diminished remyelination potential in progressive multiple sclerosis. *Proc Natl Acad Sci U S A* 2019; **116**: 9030-9039 [PMID: 30910981 DOI: 10.1073/pnas.1818348116]
39 **Coppé JP**, Patil CK, Rodier F, Sun Y, Muñoz DP, Goldstein J, Nelson PS, Desprez PY, Campisi J. Senescence-associated secretory phenotypes reveal cell-nonautonomous functions of oncogenic RAS and the p53 tumor suppressor. *PLoS Biol* 2008; **6**: 2853-2868 [PMID: 19053174 DOI: 10.1371/journal.pbio.0060301]
40 **Razdan N**, Vasilopoulos T, Herbig U. Telomere dysfunction promotes transdifferentiation of human fibroblasts into myofibroblasts. *Aging Cell* 2018; **17**: e12838 [PMID: 30244523 DOI: 10.1111/acel.12838]
41 **Birch J**, Barnes PJ, Passos JF. Mitochondria, telomeres and cell senescence: Implications for lung

ageing and disease. *Pharmacol Ther* 2018; **183**: 34-49 [PMID: 28987319 DOI: 10.1016/j.pharmthera.2017.10.005]

42 **Vasileiou PVS**, Evangelou K, Vlasis K, Fildisis G, Panayiotidis MI, Chronopoulos E, Passias PG, Kouloukoussa M, Gorgoulis VG, Havaki S. Mitochondrial Homeostasis and Cellular Senescence. *Cells* 2019; **8** [PMID: 31284597 DOI: 10.3390/cells8070686]

43 **Correia-Melo C**, Passos JF. Mitochondria: Are they causal players in cellular senescence? *Biochim Biophys Acta* 2015; **1847**: 1373-1379 [PMID: 26028303 DOI: 10.1016/j.bbabio.2015.05.017]

44 **Houtkooper RH**, Cantó C, Wanders RJ, Auwerx J. The secret life of NAD+: an old metabolite controlling new metabolic signaling pathways. *Endocr Rev* 2010; **31**: 194-223 [PMID: 20007326 DOI: 10.1210/er.2009-0026]

45 **Cantó C**, Houtkooper RH, Pirinen E, Youn DY, Oosterveer MH, Cen Y, Fernandez-Marcos PJ, Yamamoto H, Andreux PA, Cettour-Rose P, Gademann K, Rinsch C, Schoonjans K, Sauve AA, Auwerx J. The NAD(+) precursor nicotinamide riboside enhances oxidative metabolism and protects against high-fat diet-induced obesity. *Cell Metab* 2012; **15**: 838-847 [PMID: 22682224 DOI: 10.1016/j.cmet.2012.04.022]

46 **Johnson S**, Imai SI. NAD $^+$ biosynthesis, aging, and disease. *F1000Res* 2018; **7**: 132 [PMID: 29744033 DOI: 10.12688/f1000research.12120.1]

47 **Shyh-Chang N**, Ng HH. The metabolic programming of stem cells. *Genes Dev* 2017; **31**: 336-346 [PMID: 28314766 DOI: 10.1101/gad.293167.116]

48 **Yoshino J**, Baur JA, Imai SI. NAD^+ Intermediates: The Biology and Therapeutic Potential of NMN and NR. *Cell Metab* 2018; **27**: 513-528 [PMID: 29249689 DOI: 10.1016/j.cmet.2017.11.002]

49 **Zhang H**, Ryu D, Wu Y, Gariani K, Wang X, Luan P, D'Amico D, Ropelle ER, Lutolf MP, Aebersold R, Schoonjans K, Menzies KJ, Auwerx J. NAD^+ repletion improves mitochondrial and stem cell function and enhances life span in mice. *Science* 2016; **352**: 1436-1443 [PMID: 27127236 DOI: 10.1126/science.aaf2693]

50 **Igarashi M**, Miura M, Williams E, Jaksch F, Kadowaki T, Yamauchi T, Guarente L. NAD^+ supplementation rejuvenates aged gut adult stem cells. *Aging Cell* 2019; **18**: e12935 [PMID: 30917412 DOI: 10.1111/acel.12935]

51 **Lees JG**, Gardner DK, Harvey AJ. Nicotinamide adenine dinucleotide induces a bivalent metabolism and maintains pluripotency in human embryonic stem cells. *Stem Cells* 2020; **38**: 624-638 [PMID: 32003519 DOI: 10.1002/stem.3152]

Published by **Baishideng Publishing Group Inc**
7041 Koll Center Parkway, Suite 160, Pleasanton, CA 94566, USA
Telephone: +1-925-3991568
E-mail: bpgoffice@wjgnet.com
Help Desk: https://www.f6publishing.com/helpdesk
https://www.wjgnet.com